Velocity Vector Roll Control of a Fighter Aircraft with Multi-axis Thrust Vectoring Controls

Özgür Atesoglu* and M. Kemal Özgören**

*Aselsan Inc., MGEO, Akyurt, 06750
Ankara, Turkey (Tel: (90)-312-847 5300; e-mail: oatesoglu@mgeo.aselsan.com.tr).
**Middle East Technical University, Dept. of Mechanical Eng., 06531
Ankara, Turkey, (e-mail: ozgoren@metu.edu.tr)

Abstract: This paper emphasizes the challenging problem of rapid maneuvering flight control and specifically concentrated on the *velocity vector roll maneuver*. The development of automatic flight control system for rapid aircraft maneuvering requires nonlinear and coupled modeling. For that purpose a nonlinear compact, twin engine multi-axis thrust vector controlled, fighter aircraft model is built. The model includes the coupled Newtonian kinematics/dynamics, nonlinear aerodynamics, engine and thrust vectoring paddles, and, sensor models. The nonlinear controller design is based on time scale separation between the velocity vector orientation angles and the body angular velocity components. The controller is designed to command the desired velocity vector attitude angles and conduct the angle of attack, side slip angle stabilization/control features. This is effectively done by blending the aerodynamic and thrust vectoring control effectors. The performance of the proposed velocity vector roll controller is simulated in a velocity vector roll maneuver scenario and demonstrated for the mentioned fighter aircraft model.

Keywords: velocity vector roll control, nonlinear dynamic inversion, thrust vectoring control.

1. INTRODUCTION

The emerging high angle of attack capabilities of modern tactical aircraft have focused an inherent attention on the problem of making rapid roll maneuvers which are extremely important in close air combat and post-stall flight maneuvers. The successive rapid roll maneuvers are achieved by the careful suppression of the sideslip and the rates of the angle of attack and the total velocity of the aircraft throughout the whole maneuver. Since, during that maneuver, the orientation of the aircraft with respect to the velocity vector axis remains constant, and it turns a whole revolution around the same axis, it is termed as the velocity vector roll maneuver. An illustrative sketch for that maneuver is shown in Fig. 1.
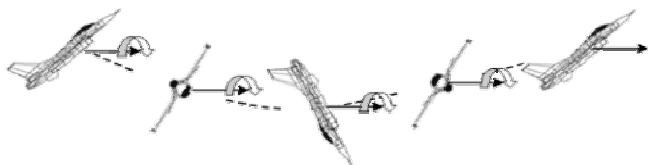
Fig. 1. Illustration of a velocity vector roll maneuver.

The velocity vector roll maneuver is also known as a milestone to demonstrate the performance of a successful rapid maneuvering fighter aircraft, and, adopted as an effective maneuver with its combat advantages. The operational significance of this maneuver is to allow the fighter aircraft to quickly slew and point its nose relatively faster than a combination of conventional pull-up first and then turn maneuver. Hence, realizing the maneuver successfully and minimizing the pilot induced inabilities arising from the external environment, automatic rapid maneuvering controllers are extensively studied in the literature (Enns 1992, Bugajski 1992).

Designing a rapid velocity vector roll maneuver controller is difficult for a couple of reasons. First, it shall be noted that both the aerodynamic and the thrust vectoring control actuators provide moments primarily about the directional (body x-axis) of the aircraft rather than the velocity vector axis. Thus, the angle of attack (α) and the side slip angle (β) of the aircraft shall be controlled during the maneuver.

Especially, having large side slip angles through and at the end of the maneuver will result in an unsuccessful velocity vector roll maneuver that the nose of the aircraft will not be pointed to a desired direction (Boyum 1995, Pachter 1997). Another major difficulty arises from the strong coupling of the longitudinal and lateral/directional motions due to the coupled kinematics of the maneuver itself. The velocity vector roll maneuvers necessitate high amplitude motions for the flight variables, and thus, standard linear aircraft models and linear flight control systems, based on small perturbation hypothesis and separation of the longitudinal and lateral/directional channels, cannot be used. The kinematic/dynamic nonlinearities shall be included in the aircraft model that is to be used in the velocity vector roll controller design.

The objective of this paper is to design a nonlinear velocity vector roll controller to operate on the high amplitude velocity vector roll angles of the aircraft at moderate/high angle of attack flights. This paper is a sequel to the previous work (Atesoglu 2007) in which the nonlinear plant model of the twin engine fighter aircraft, with aerodynamic and thrust vectoring controls, was established, the nonlinear controller design, based on time scale separation between the aircraft body attitude angles (ϕ, θ, ψ) and the body angular velocity components (p, q, r), was evoked, the blending strategy for the aerodynamic and thrust vector control surfaces was conducted and the robustness of the designed controller was analyzed.

In the paper the nonlinear kinematics of the velocity vector attitude is presented and the kinematic relations, both for the angle and angular velocity representations, between the aircraft body attitude angles and the velocity vector attitude angles ($\gamma_x, \gamma_y, \gamma_z$) are derived. Further, the previously designed controller is modified to operate on the velocity vector attitude angles and the desired angle of attack (α), side slip angle (β) stabilization and control features are added. The performance of the designed velocity vector roll controller is demonstrated in a velocity vector roll maneuver scenario simulation done for the mentioned twin engine fighter aircraft with aerodynamic and thrust vectoring controls (Atesoglu 2007).

2. NONLINEAR DYNAMIC MODEL

In the dynamic modeling the aircraft is assumed to be rigid with constant mass and density and symmetric about its *x-z* plane. It is also assumed that the un-deflected thrust forces of each of the two engines act parallel to the longitudinal body axis. However, it can be deviated as desired by using the thrust-vectoring paddles. As for the modeling two reference frames are defined as the earth fixed reference frame (assumed to be inertial) and the body fixed reference frame attached to the mass center of the aircraft. The two thrust vectoring control forces (i.e. the forces obtained by thrust deviations) in the TVC phase are denoted by $\vec{F}_L$ and $\vec{F}_R$. They are applied at arbitrary directions at different locations, i.e. $\vec{r}_{be_L}$ and $\vec{r}_{be_R}$. The position of the aircraft with respect to the earth fixed reference frame is defined by $\vec{r}_{ob}$. The mentioned reference frames, actuation forces with their locations, and the aerodynamic forces and moments on the aircraft are shown in Fig. 2.
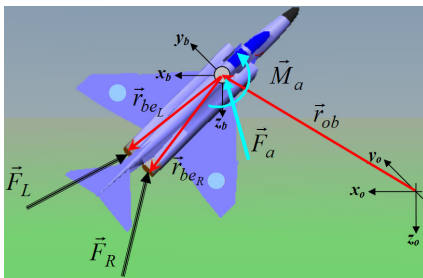
Fig. 2. The position, force, moment and frame definitions.

As it is presented in (Atesoglu 2007) the Newton-Euler equations describing the rigid body motion of the aircraft can be combined into a single matrix equation:

$$\begin{bmatrix} [\dot{u}\ \dot{v}\ \dot{w}]^{\mathrm{T}} \\ [\dot{p}\ \dot{q}\ \dot{r}]^{\mathrm{T}} \end{bmatrix} = \overline{F} + \hat{G}\begin{bmatrix} \overline{F}_L^{(b)} \\ \overline{F}_R^{(b)} \end{bmatrix} + \hat{H}\begin{bmatrix} \overline{F}_a^{(b)} \\ \overline{M}_a^{(b)} \end{bmatrix} \qquad (1)$$

Here the matrices $\overline{F}$, $\hat{G}$, and $\hat{H}$ are:

$$\overline{F} = \begin{bmatrix} -\widetilde{\omega}_{b/o}^{(b)}\overline{v}_{b/o}^{(b)} + g\hat{C}^{(b,o)}\overline{u}_3 \\ -\hat{J}^{-1}\widetilde{\omega}_{b/o}^{(b)}\hat{J}\overline{\omega}_{b/o}^{(b)} \end{bmatrix}, \quad \hat{G} = \begin{bmatrix} \hat{I}/m & \hat{I}/m \\ \hat{J}^{-1}\widetilde{r}_{be_L}^{(b)} & \hat{J}^{-1}\widetilde{r}_{be_R}^{(b)} \end{bmatrix}, \text{ and,}$$

$$\hat{H} = \begin{bmatrix} \hat{I}/m & 0 \\ 0 & \hat{J}^{-1} \end{bmatrix}.$$

Here, u, v, w are the translational velocity components expressed in the body fixed frame and p, q, r are the angular velocity components expressed in the body fixed reference frame. Here, $\overline{u}_1, \overline{u}_2, \overline{u}_3$ are defined as the unit vectors along the body frame axes and $\hat{R}_k(\theta)$ is defined as the rotation matrix of angle θ about the kth axis of a reference frame. Thus, $\overline{F}_L^{(b)} = T_L\hat{R}_3(\psi_L)\hat{R}_2(\theta_L)\overline{u}_1$, $\overline{F}_R^{(b)} = T_R\hat{R}_3(\psi_R)\hat{R}_2(\theta_R)\overline{u}_1$ are the thrust force vectors of the two engines with magnitudes T_L and T_R. Their azimuth and elevation angles with respect to the body fixed reference system are denoted by the pairs { ψ_L, ψ_R} and { θ_L, θ_R}. The aerodynamic force and moment vector components expressed in the body fixed frame, created on the aircraft during its flight, are denoted with $\overline{F}_a^{(b)}, \overline{M}_a^{(b)}$. In the equations the mass of the aircraft is denoted with m, the inertia tensor of the aircraft is expressed by the matrix $\hat{J}$ in the body fixed frame, and the earth gravity field vector is denoted with g. Also, $\hat{C}^{(o,b)}$ is the rotation matrix from the earth fixed reference frame to the body fixed reference frame composed by three successive rotations defined by the *Euler angles*, i.e. $\hat{C}^{(o,b)} = \hat{R}_3(\psi)\hat{R}_2(\theta)\hat{R}_1(\phi)$. The angular velocity of the aircraft with respect to the earth fixed reference frame expressed in the body fixed frame is denoted by $\overline{\omega}_{b/o}^{(b)}$ and the translational velocity of the aircraft with respect to the earth fixed reference frame expressed in the body fixed frame is denoted by $\overline{v}_{b/o}^{(b)}$.

2.1. The Nonlinear Aerodynamic Model

The aerodynamic data, used in the simulation model, is gathered assuming that the ground effect is absent, the landing gears are retracted, and, there are no external stores. The nonlinear aerodynamics is modeled in terms of polynomial functions that involve $\delta_e, \delta_a, \delta_r$, α, β, p, q, r (Garza 2003). Polynomial fits for each of the non-dimensional coefficients are valid over $-15^\circ \leq \alpha \leq 55^\circ$. Aerodynamic coefficients are referenced to an assumed center of gravity location originated from the technical documentary of the aircraft. The control surface deflections

are assumed to be limited as: $-21° \leq \delta_e \leq 7°$, $-16° \leq \delta_a \leq 16°$, $-30° \leq \delta_r \leq 30°$. The equations of some of the coefficients used in the model, i.e. C_X, C_l, for $-15° \leq \alpha \leq 15°$ are presented in Eq. (2).

$$C_X = -0.0434 + 2.39\times10^{-3}\alpha + 2.53\times10^{-5}\beta^2 - 1.07\times10^{-6}\alpha\beta^2 + 9.5\times10^{-4}\delta_e$$
$$-8.5\times10^{-7}\delta_e\beta^2 + \left(\frac{180q\bar{c}}{\pi 2V_t}\right)\left(8.73\times10^{-3} + 0.001\alpha - 1.75\times10^{-4}\alpha^2\right)$$

$$C_l = -5.98\times10^{-4}\beta - 2.83\times10^{-4}\alpha\beta + 1.51\times10^{-5}\alpha^2\beta$$
$$-\delta_a\left(6.1\times10^{-4} + 2.5\times10^{-5}\alpha - 2.6\times10^{-6}\alpha^2\right)$$
$$-\delta_r\left(-2.3\times10^{-4} + 4.5\times10^{-6}\alpha\right)$$
$$+\left(\frac{180b}{\pi 2V_t}\right)\left(-4.12\times10^{-3}p - 5.24\times10^{-4}p\alpha + 4.36\times10^{-5}p\alpha^2\right.$$
$$\left.+4.36\times10^{-4}r + 1.05\times10^{-4}r\alpha + 5.24\times10^{-5}r\delta_e\right) \qquad (2)$$

2.2. The Engine and TVC Paddle Model

Each engine of the aircraft is modeled as a first order dynamic system with the following response equation to a commanded power demand: $\tau_{eng}\dot{P}_a + P_a = P_c$. Here P_a is the actual power output and P_c is the commanded power demand. P_c is a function of the throttle position (δ_{th}) and the engine time constant τ_{eng} is scheduled to achieve a satisfactory engine dynamics. The thrust force T of each engine is typically determined as a function of the actual power, the altitude, and the Mach number for idle, military, and maximum power settings (Nguyen 1979).

The fighter aircraft considered in this study does not originally have the capability of thrust-vectoring. Therefore, it is assumed that it is also virtually fitted with a similar thrust-vectoring system as those that are used for the *X-31A* and NASA *F-18 HARV* aircraft that employs three post-exit vanes radially displaced about their axi-symmetric nozzles (Bowers 1991). Thus, a jet turning envelope similar to that of the HARV aircraft is generated for the modeling purposes.
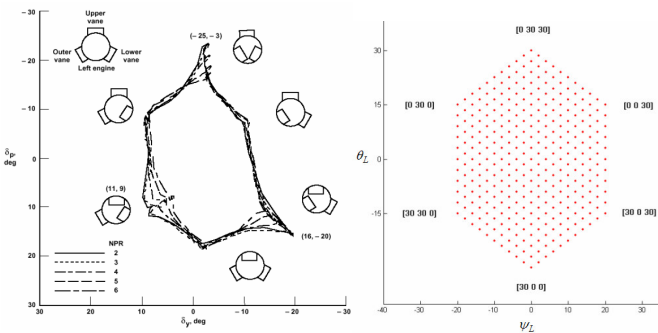
Fig. 3. Maximum jet turning angle envelopes for NASA F-18 HARV (left) and the mode under study (right).

The virtually fitted thrust-vectoring system has three thrust-vectoring paddles on each of the right and left engine nozzle exits. Therefore, thrusts of the right and left engines can be

deviated individually to form a multi-axis TVC. Since the shape of this envelope is hexagonal the maximum deflections of the three paddles lead to different maximum values of lateral and longitudinal thrust deviations, i.e. $30°$ for pitch and $20°$ for yaw deviations (Fig. 3).

2.3. The Aircraft Sensors Model

Here, the sensor models for the flight variables, i.e. ϕ, θ, ψ, p, q, r, α, β, used in the velocity vector roll controller are also conducted. The mentioned flight variables are measured by the *inertial navigation system* (*INS*), *inertial measurement unit* (*IMU*) and the *flow angle sensors*. The error sources on these sensors have both deterministic and stochastic nature. These errors arise due to the bias, bias instability, scale factor and misalignments. Typically, in controller design studies, bias and the bias instability are taken into account.

Any flight variable sensor is modeled with $s_m = s + b_s + n_s$ and $\tau_{ws}\dot{n}_s + n_s = w_s$. Here, s is any flight variable, s_m is the measured flight variable, b_s is the constant bias term, and, n_s is the stochastic bias instability signal. The bias instability signal is modeled as it is generated from the first order Gauss-Markov process filters using the time constant τ_{ws} and white Gaussian noise signal w_s. Also, the sensor dynamic models are introduced into the simulations as $\tau_s\dot{s}' + s' = s$. Here τ_s is the time constant of the sensor of the associated flight variable s, and, s' is the lagged measurement.

Due to the measurement techniques the coupling of the flow angle (α, β) measurements are more significant than the others. Thus, the measurements in the longitudinal plane of motion are coupled with the ones in the lateral plane and show up as undesired errors (Haering 1995). Hence, during the simulations of the velocity vector roll control the flow angles measurements are modeled by introducing the cross-coupling effect of flow angles.

3. NONLINEAR CONTROLLER DESIGN

In this study the plant model is built to use the aerodynamic control effectors, i.e. elevator, aileron, rudder deflections, together with thrust vectoring control effectors. The TVC control surfaces are the six TVC paddles on the left and the right engine nozzle exits, i.e. $\delta_{L(1,2,3)}$ and $\delta_{R(1,2,3)}$. Further, the left and right engine thrusts are controlled by using the engine throttle deflections, i.e. $\delta_{Lth}, \delta_{Rth}$.

3.1. Controller Design Using the Thrust Vectoring Controls

The thrust vectoring controller is designed to be started whenever the aerodynamic controllers lose their effectiveness. Therefore, when the thrust vector controller is turned on, the aerodynamic controller is turned off and the aerodynamic control effectors are retracted to their neutral positions. In such a case, the aircraft is controlled only by

using the total thrusts T_L and T_R created by the two engines and the thrust vector deviation angle pairs $\{\psi_L, \theta_L\}$ and $\{\psi_R, \theta_R\}$. In the case of thrust vectoring controls, using the dynamic inversion control law, the command values for the forces to be created by the left and right engines can be calculated using the following equation for a commanded acceleration state of the aircraft:

$$
\begin{bmatrix} \overline{F}_c^{(b)} \\ \overline{M}_c^{(b)} \end{bmatrix} = \hat{H}^{-1} \left\{ \begin{bmatrix} [\dot{u}_c\ \dot{v}_c\ \dot{w}_c]^{\mathrm{T}} \\ [\dot{p}_c\ \dot{q}_c\ \dot{r}_c]^{\mathrm{T}} \end{bmatrix} - \overline{F} - \hat{H} \begin{bmatrix} \overline{F}_a^{(b)} \\ \overline{M}_a^{(b)} \end{bmatrix} \right\}
\tag{3}
$$

Here, $\overline{F}_c^{(b)}$ and $\overline{M}_c^{(b)}$ are the necessary force and moment vectors in order to realize the commanded accelerations completely. As noted, the coefficient matrix in Eq. (3) is rank-deficient. Therefore, the consistency of this equation can be satisfied by allowing freedom for certain components of $\overline{F}_c^{(b)}$ and $\overline{M}_c^{(b)}$. Thus, $\overline{F}_c^{(b)}$ and $\overline{M}_c^{(b)}$ are determined by "careful distribution" of the acceleration commands, i.e. $\dot{u}_c, \dot{v}_c, \dot{w}_c$, and, $\dot{p}_c, \dot{q}_c, \dot{r}_c$, to $\overline{F}_L^{(b)}$ and $\overline{F}_R^{(b)}$. Thus, the spherical components of them, i.e. $\{T_L, \psi_L, \theta_L\}$ and $\{T_R, \psi_R, \theta_R\}$, can be determined.

3.2. Controller Design Using the Aerodynamic Controls

As for the aerodynamic controls the command values for the aerodynamic forces and moments should be calculated. In this case, for commanded accelerations and un-deflected TVC paddles, following equation can be written:

$$
\begin{bmatrix} \overline{F}_{ac}^{(b)} \\ \overline{M}_{ac}^{(b)} \end{bmatrix} = \hat{H}^{-1} \left\{ \begin{bmatrix} [\dot{u}_c\ \dot{v}_c\ \dot{w}_c]^{\mathrm{T}} \\ [\dot{p}_c\ \dot{q}_c\ \dot{r}_c]^{\mathrm{T}} \end{bmatrix} - \overline{F} - \hat{G} \begin{bmatrix} [T_L\ 0\ 0]^{\mathrm{T}} \\ [T_R\ 0\ 0]^{\mathrm{T}} \end{bmatrix} \right\}
\tag{4}
$$

For the velocity vector roll controller the aerodynamic control surface deflection commands, i.e. $\delta_{ac}, \delta_{ec}, \delta_{rc}$, are found from $\overline{M}_{ac}^{(b)}$. Using the aerodynamic moment coefficients in Eq. (5) the aerodynamic moments are expressed by $M_{ax}^{(b)} = (Q_d S b) C_l$, $M_{ay}^{(b)} = (Q_d S \overline{c}) C_m$, and, $M_{az}^{(b)} = (Q_d S b) C_n$. Here, Q_d is the dynamic pressure, S is the surface area of the wing planform, $\overline{c}$ is the mean chord length and b is the span of the wing. Here note that, C_l, C_m, C_n are:

$$
C_l = C_l'(\alpha, \beta, p, q, r) + C_{l\delta_a}(\alpha, \beta)\delta_a + C_{l\delta_r}(\alpha, \beta)\delta_r
\tag{5.a}
$$
$$
C_m = C_m'(\alpha, \beta, p, q, r) + C_{m\delta_e}(\alpha, \beta)\delta_e
\tag{5.b}
$$
$$
C_n = C_n'(\alpha, \beta, p, q, r) + C_{n\delta_a}(\alpha, \beta)\delta_a + C_{n\delta_r}(\alpha, \beta)\delta_r
\tag{5.c}
$$

Thus, the commanded aerodynamic control surface deflections for $\dot{p}_c, \dot{q}_c, \dot{r}_c$ and $\overline{M}_{ac}^{(b)}$ can be calculated:

$$
\begin{bmatrix} \delta_{ac} \\ \delta_{ec} \\ \delta_{rc} \end{bmatrix} = \begin{bmatrix} C_{l\delta_a} & 0 & C_{l\delta_r} \\ 0 & C_{m\delta_e} & 0 \\ C_{n\delta_a} & 0 & C_{n\delta_r} \end{bmatrix}^{-1} \begin{bmatrix} M_{axc}^{(b)}/(Q_d S b) - C_l' \\ M_{ayc}^{(b)}/(Q_d S \overline{c}) - C_m' \\ M_{azc}^{(b)}/(Q_d S b) - C_n' \end{bmatrix}
\tag{6}
$$

3.3. Velocity Vector Roll Controller Design

In order to command the attitude of the aircraft's velocity vector the orientation angles of the velocity of the aircraft should be controlled. Thus, the velocity vector roll angle and the flight path angles ($\gamma_x, \gamma_y, \gamma_z$) shall be calculated. Recall that by using the Euler angles the rotation matrix from the earth fixed reference frame to the body fixed reference frame can be defined, i.e. $\hat{C}^{(o,b)}$. Similarly, by using $\gamma_z, \gamma_y, \gamma_x$ the rotation matrix from the earth fixed reference frame to the wind axis reference frame can be defined as $\hat{C}^{(o,w)} = \hat{R}_3(\gamma_z)\hat{R}_2(\gamma_y)\hat{R}_1(\gamma_x)$. Also, two successive rotations, made by angle of attack and side slip angles, defines the rotation sequence from the body fixed reference frame to the wind axis frame: $\hat{C}^{(b,w)} = \hat{R}_2(-\alpha)\hat{R}_3(\beta)$. Hence, writing $\hat{C}^{(o,w)} = \hat{C}^{(o,b)}\hat{C}^{(b,w)}$, the velocity vector orientation angles can be calculated: $\gamma_x = \tan^{-1}(\hat{C}_{32}^{(o,w)}, \hat{C}_{33}^{(o,w)})$, $\gamma_y = \sin^{-1}(-\hat{C}_{31}^{(o,w)})$, and, $\gamma_z = \tan^{-1}(\hat{C}_{21}^{(o,w)}, \hat{C}_{11}^{(o,w)})$. The angular velocity of the aircraft with respect to the earth fixed reference frame expressed at wind axis coordinates can be found by the time derivative of $\hat{C}^{(o,w)} = \hat{C}^{(o,b)}\hat{C}^{(b,w)}$ and $\hat{C}^{(o,w)} = \hat{R}_3(\gamma_z)\hat{R}_2(\gamma_y)\hat{R}_1(\gamma_x)$ at the same time. Thus, calculating the column vector representation of that angular velocity ($\overline{\omega}_{w/o}^{(o)}$) from both ways and equating them the time derivatives of velocity vector orientation angles can be found:

$$
\begin{aligned}
\overline{\omega}_{w/o}^{(o)} &= \hat{C}^{(o,b)}\overline{\omega}_{b/o}^{(b)} - \dot{\alpha}\hat{C}^{(o,b)}\overline{u}_2 + \dot{\beta}\hat{C}^{(o,b)}\hat{R}_2(-\alpha)\overline{u}_3 \\
&= \dot{\gamma}_z\overline{u}_3 + \dot{\gamma}_y\hat{R}_3(\gamma_z)\overline{u}_2 + \dot{\gamma}_x\hat{R}_3(\gamma_z)\hat{R}_2(\gamma_y)\overline{u}_1
\end{aligned}
\tag{7.a}
$$

$$
\begin{bmatrix} \dot{\gamma}_x \\ \dot{\gamma}_y \\ \dot{\gamma}_z \end{bmatrix} = \hat{C}_T^{(w,o)}\hat{C}^{(o,b)} \begin{bmatrix} p \\ q \\ r \end{bmatrix} + \begin{bmatrix} -\hat{C}_T^{(w,o)}\hat{C}^{(o,b)}\overline{u}_2 \\ \hat{C}_T^{(w,o)}\hat{C}^{(o,b)}\hat{R}_2(-\alpha)\overline{u}_3 \end{bmatrix}^{\mathrm{T}} \begin{bmatrix} \dot{\alpha} \\ \dot{\beta} \end{bmatrix}
\tag{7.b}
$$

$$
\hat{C}_T^{(w,o)} = \begin{bmatrix} c\gamma_z/c\gamma_y & s\gamma_z/c\gamma_y & 0 \\ -s\gamma_z & c\gamma_z & 0 \\ c\gamma_z t\gamma_y & s\gamma_z t\gamma_y & 1 \end{bmatrix}
\tag{7.c}
$$

Here, c, s, t are used as short hand notations of cos, sin and tan functions respectively. Note that, $\hat{C}_T^{(w,o)}$ is singular for $\gamma_y = \pm\pi/2$, and thus, at that value direct conversion between $\dot{\gamma}_x, \dot{\gamma}_y, \dot{\gamma}_z$ and $p, q, r, \dot{\alpha}, \dot{\beta}$ cannot be written.

The aim of the velocity vector controller is to control the velocity vector roll and angle of attack and side slip angles. Thus, $\overline{F}_c^{(b)}, \overline{M}_c^{(b)}$ shall be calculated using the commanded

accelerations as shown in Eq. (4). In order to calculate the commanded angular accelerations the commanded body angular velocities (p_c, q_c, r_c) should be calculated. Thus, the controller is separated into two different time scales. First, the rates of the commanded velocity vector roll angle and flight path angles ($\dot{\gamma}_{xc}, \dot{\gamma}_{yc}, \dot{\gamma}_{zc}$) are generated. Then, the commanded body angular velocities ($\dot{p}_c, \dot{q}_c, \dot{r}_c$) are calculated by using these values. Conventionally, $\dot{\gamma}_{xc}, \dot{\gamma}_{yc}, \dot{\gamma}_{zc}$ are called the "slow" while $\dot{p}_c, \dot{q}_c, \dot{r}_c$ are called "fast" time scales. Defining the desired velocity vector roll and the flight path angles as $\gamma_{xd}, \gamma_{yd}, \gamma_{zd}$, the error vector, i.e. the difference between the desired (d) and the actual values of the velocity vector attitude angles is represented as

$$\bar{e}_r(t) = \left[(\gamma_{xd}(t) - \gamma_x(t))(\gamma_{yd}(t) - \gamma_y(t))(\gamma_{zd}(t) - \gamma_z(t)) \right]^{\mathrm{T}} \quad (8)$$

Processing the error ($\bar{e}_r(t)$) in a proportional and integral (PI) controller structure augmented with feed-forward rate commands, the commanded velocity vector angular velocities can be calculated:

$$\begin{bmatrix} \dot{\gamma}_{xc}(t) \\ \dot{\gamma}_{yc}(t) \\ \dot{\gamma}_{zc}(t) \end{bmatrix} = \hat{K}_{pr}\bar{e}_r(t) + \hat{K}_{ir}\int_0^t \bar{e}_r(t')dt' + \begin{bmatrix} \dot{\gamma}_{xd}(t) \\ \dot{\gamma}_{yd}(t) \\ \dot{\gamma}_{zd}(t) \end{bmatrix} \quad (9)$$

Here, $\hat{K}_{pr}, \hat{K}_{ir}$ are the constant gain slow dynamics controller matrices. After calculating the commanded velocity vector angular velocities p_c, q_c, r_c can be calculated by using Eq. (7.b):

$$\begin{bmatrix} p_c(t) \\ q_c(t) \\ r_c(t) \end{bmatrix} = \hat{C}^{(b,o)}\hat{C}_T^{(o,w)} \left(\begin{bmatrix} \dot{\gamma}_{xc} \\ \dot{\gamma}_{yc} \\ \dot{\gamma}_{zc} \end{bmatrix} - \begin{bmatrix} -\hat{C}_T^{(w,o)}\hat{C}^{(o,b)}\bar{u}_2 \\ \hat{C}_T^{(w,o)}\hat{C}^{(o,b)}R_2(-\alpha)\bar{u}_3 \end{bmatrix}^{\mathrm{T}} \begin{bmatrix} \dot{\alpha} \\ \dot{\beta} \end{bmatrix} \right) \quad (10)$$

Once p_c, q_c, r_c are calculated they are fed to the second, i.e. fast, segment of the controller. At this stage $\bar{e}_{av}(t)$ is defined as the difference between the commanded (c) and the actual values of the body angular velocity components:

$$\bar{e}_{av}(t) = \left[(p_c(t) - p(t))(q_c(t) - q(t))(r_c(t) - r(t)) \right]^{\mathrm{T}} \quad (11)$$

Processing the error ($\bar{e}_{av}(t)$) in a proportional (P) controller structure, the commanded angular accelerations $\dot{p}_c, \dot{q}_c, \dot{r}_c$ can be calculated from $[\dot{p}_c(t)\,\dot{q}_c(t)\,\dot{r}_c(t)]^T = \hat{K}_d\bar{e}_{av}(t)$. Here, $\hat{K}_d$ is the constant gain fast dynamics controller matrix. Hence, calculating $\dot{p}_c, \dot{q}_c, \dot{r}_c$, $\overline{M}_c^{(b)}$ and $\overline{M}_{ac}^{(b)}$ in Eq. (3) and Eq. (4) can be calculated. Applying the careful distribution of the angular accelerations, due to the rank deficiency of the

equations mentioned in Section 3.1, $\overline{F}_{Lc}^{(b)}, \overline{F}_{Rc}^{(b)}$ and $\{T_{Lc}, \psi_{Lc}, \theta_{Lc}\}$, $\{T_{Rc}, \psi_{Rc}, \theta_{Rc}\}$ (and the throttle deflections and the six thrust-vectoring paddle deflections) can be found. The velocity vector controller block diagram is shown in Fig. 4 and Fig. 5.
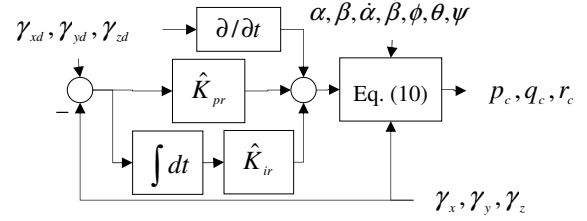
Fig. 4. Angular velocity command generation block diagram, i.e. the slow dynamics.
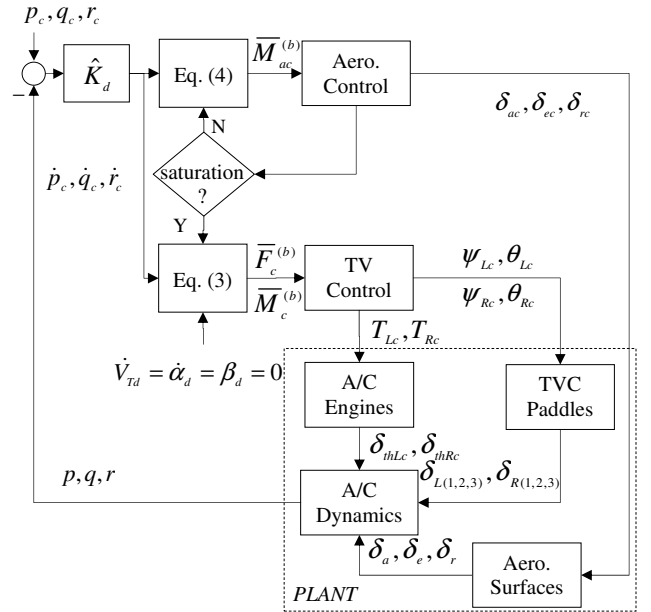
Fig. 5. Angular velocity controller block diagram with aerodynamic and the thrust vectoring control effectors.

The block diagram in Fig. 5 shows the angular velocity controller, i.e. the fast dynamics, designed for velocity vector roll controller. In the controller the thrust vectoring and the aerodynamic controls are used together. In order to achieve the desired commands, primarily, the conventional aerodynamic control effectors are used. However, they are continuously monitored to be aware of mechanical saturation. Whenever any aerodynamic control surface is saturated it is rapidly commanded to its neutral position. Hence, the desired commands are realized by only using the thrust vectoring controls until an unsaturated aerodynamic control surface command is generated.

4. THE NUMERICAL SIMULATIONS

The velocity vector roll maneuver simulation is started from the initial condition at which the fighter aircraft is at 10,000 m altitude at 0.8 Mach and at $\theta_0 = 10°$ climb. Applying the

trim algorithm presented in (Atesoglu 2008) the equilibrium points at the specified flight condition are found as $\beta_0 = \delta_{a0} = \delta_{r0} = 0°$, $T_0 = 26,314\,\text{N}$, $\delta_{Lth} = \delta_{Rth} = 0.85$, and, $\alpha_0 = 3.11°$, $\delta_{e0} = -2.19°$,.

The velocity vector roll angle is commanded to perform a velocity vector roll full turn ($0°$ to $360°$) in 19 seconds. Here, a hybrid controller is operated to realize the commanded velocity vector roll angle of attack and side slip angle. When the velocity vector roll maneuver is started the angle of attack and the side slip angles are stabilized by regulating $\dot{\alpha}, \dot{\beta}$ for 9 seconds. Consequently, at the last 10 seconds of the maneuver the angle of attack is commanded to $10°$ and the side slip angle is commanded to $0°$. The numerical simulations are supported with the visual interpretation tool generated by using the VRML tool. Hence, the aircraft's motion during the simulated velocity vector roll maneuver can be shown in the following figure.
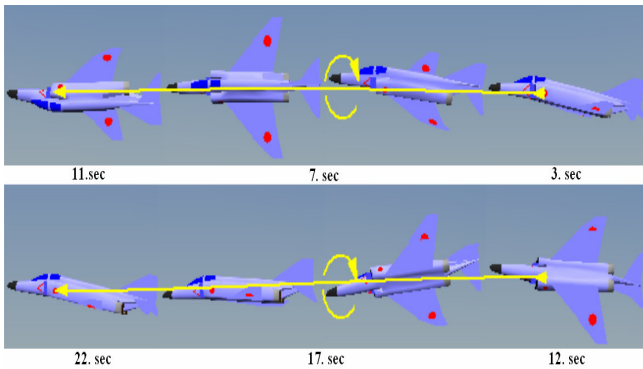
Fig. 6. Visual interpretation of the simulated velocity vector roll maneuver.

The time histories of the total velocity, angle of attack, side slip angle, and, the velocity vector roll, pitch and yaw angles for the simulated maneuver are shown in the following figures.
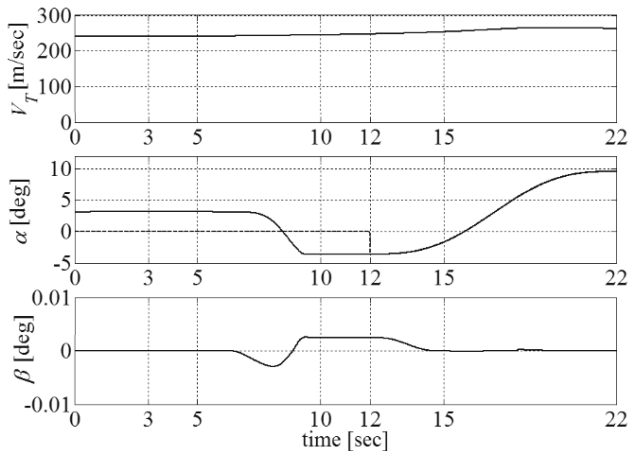
Fig. 7. The time histories of V_T, α, β for the simulated velocity vector roll maneuver.

Throughout the maneuver the aerodynamic control surfaces are saturated at different instants. The aileron, elevator and rudder are saturated for 3.2, 1.9, and, 3.8 seconds respectively in total. Nevertheless, the participation of the aerodynamic and thrust vectoring controls is successful. Whenever the aerodynamic control surfaces are saturated the control is handed over to TVC and the maneuver is continued smoothly.
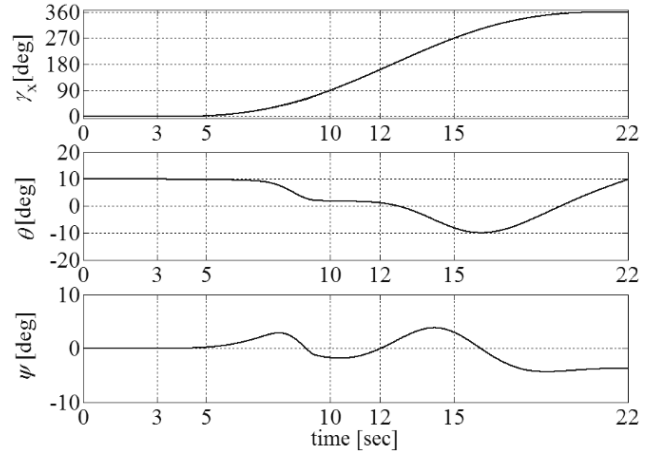
Fig. 8. The time histories of γ_x, θ, ψ for the simulated velocity vector roll maneuver.

5. REFERENCES

Atesoglu, Ö., Özgören, M.K. (2007). High-alpha Flight Maneuverability Enhancement of a Fighter Aircraft Using Thrust-Vectoring Control. *Journal of Guidance, Control and Dynamics*, Vol. 30, No. 5, pp. 1480-1493.

Bowers, A., Noffz, G., Grafton, S.B., Mason, M.L., Peron, L.R. (1991). Multi-axis Thrust Vectoring Using Axi-symmetric Nozzles and Post-exist Vanes on an F-18 Configuration Vehicle. NASA-TM-101741, Dryden Flight Research Facility, Edwards, CA.

Boyum, K.E., Pachter, M., Houpis, C.H. (1995). High Angle of Attack Velocity Vector Rolls. *Control Engineering Practice*. Vol. 3, Issue 8, pp. 1087-1093.

Bugajski, J.D., and Enns, F.D. (1992). Nonlinear Control Law with Application to High Angle of Attack Flight. *Journal of Guidance, Control, and Dynamics*. Vol. 15, No. 3, pp. 761–767.

Garza, F.R., Morelli, E.A. (2003). A Collection of Nonlinear Aircraft Simulations in MATLAB. NASA/TM-2003-212145.

Haering, E.A. (1995). Airdata Measurement and Calibration. NASA Technical Memorandum, 104316. NASA Dryden Flight Research Center, Edwards, CA.

Nguyen, L.T., Ogburn, M.E., Gilbert, W.P., Kibler, K.S., Brown, P.W., Deal, P.L. (1979). Simulator Study of Stall/Post-Stall Characteristics of a Fighter Airplane with Relaxed Static Stability. NASA TP-1538. December.

Pachter, M., Chandler, P.R., Smith, L. (1997). Maneuvering flight control. Proceedings of American Control Conference 1997. Vol. 2, Issue 4-6, June 1997, pp. 1111-1115.